

UCLA

UCLA Previously Published Works

Title

The cellular regulators PTEN and BMI1 help mediate NEUROGENIN-3—induced cell cycle arrest

Permalink

<https://escholarship.org/uc/item/49r4v01t>

Journal

Journal of Biological Chemistry, 294(41)

ISSN

0021-9258

Authors

Solorzano-Vargas, R Sergio

Bjerknes, Matthew

Wu, S Vincent

et al.

Publication Date

2019-10-01

DOI

10.1074/jbc.ra119.008926

Copyright Information

This work is made available under the terms of a Creative Commons Attribution License, available at <https://creativecommons.org/licenses/by/4.0/>

Peer reviewed



The cellular regulators PTEN and BMI1 help mediate NEUROGENIN-3–induced cell cycle arrest

Received for publication, April 30, 2019, and in revised form, June 25, 2019. Published, Papers in Press, July 24, 2019, DOI 10.1074/jbc.RA119.008926

R. Sergio Solorzano-Vargas[‡], Matthew Bjerknes[§], S. Vincent Wu[¶], Jiafang Wang[‡], Matthias Stelzner^{||}, James C. Y. Dunn^{**}, Sangeeta Dhawan^{††}, Hazel Cheng[§], Senta Georgia^{§§}, and  Martín G. Martín^{‡1}

From the [‡]Department of Pediatrics, Division of Gastroenterology and Nutrition, Mattel Children's Hospital and the David Geffen School of Medicine, University of California, Los Angeles, Los Angeles, California 90095, the [§]Department of Medicine, Medical Sciences Building, University of Toronto, Toronto, Ontario M5S 1A8, Canada, the [¶]Veterans Affairs Greater Los Angeles Healthcare System, and Department of Medicine, University of California, Los Angeles, Los Angeles, California 90073, the ^{||}Division of General Surgery, Department of Surgery, University of California, Los Angeles, Los Angeles, California 90095, the ^{**}Division of Pediatric Surgery, Department of Surgery, Stanford University School of Medicine, Stanford, California 94305, the ^{††}Department of Translational Research and Cellular Therapeutics, City of Hope, Duarte, California 91010, and the ^{§§}Department of Pediatrics, Division of Endocrinology, Children's Hospital of Los Angeles, University of Southern California, Los Angeles, Los Angeles, California 90027

Edited by Joel M. Gottesfeld

Neurogenin-3 (NEUROG3) is a helix-loop-helix (HLH) transcription factor involved in the production of endocrine cells in the intestine and pancreas of humans and mice. However, the human NEUROG3 loss-of-function phenotype differs subtly from that in mice, but the reason for this difference remains poorly understood. Because *NEUROG3* expression precedes exit of the cell cycle and the expression of endocrine cell markers during differentiation, we investigated the effect of lentivirus-mediated overexpression of the human *NEUROG3* gene on the cell cycle of BON4 cells and various human nonendocrine cell lines. *NEUROG3* overexpression induced a reversible cell cycle exit, whereas expression of a neuronal lineage homolog, *NEUROG1*, had no such effect. In endocrine lineage cells, the cellular quiescence induced by short-term *NEUROG3* expression required cyclin-dependent kinase inhibitor 1A (CDKN1A)/p21^{CIP1} expression. Expression of endocrine differentiation markers required sustained *NEUROG3* expression in the quiescent, but not in the senescent, state. Inhibition of the phosphatase and tensin homolog (PTEN) pathway reversed quiescence by inducing cyclin-dependent kinase 2 (CDK2) and reducing p21^{CIP1} and NEUROG3 protein levels in BON4 cells and human enteroids. We discovered that *NEUROG3* expression stimulates expression of CDKN2a/p16^{INK4a} and *BMI1* proto-oncogene polycomb ring finger (*BMI1*), with the latter limiting expression of the former, delaying the onset of CDKN2a/p16^{INK4a}-driven cellular senescence. Furthermore, NEUROG3 bound to the promoters of both *CDKN1a/p21^{CIP1}* and *BMI1* genes, and BMI1 attenuated NEUROG3 binding to the *CDKN1a/p21^{CIP1}* promoter. Our findings reveal how human NEUROG3 integrates inputs from multiple signaling path-

ways and thereby mediates cell cycle exit at the onset of differentiation.

NEUROGENIN-3 (NEUROG3) is a basic helix-loop-helix (HLH)² transcription factor involved in gastrointestinal endocrine (GIE) cell lineage determination (1). In the mouse intestine, some NEUROG3⁺ cells are in cycle, but the majority are postmitotic and beginning to express early GIE cell markers (2). Similarly, in the developing mouse pancreas, mitotically active progenitor cells exit the cell cycle after the initiation of *Neurog3* expression, in a process involving the cyclin-dependent kinase inhibitor 1a (*Cdkn1a/p21^{CIP1}*) (3). Furthermore, ectopic expression of *Neurog3* in early postnatal β -cells attenuates their proliferation, and results in a reduction of total β -cell mass leading to diabetes mellitus. *Neurog3* expression seems to drive mouse pre-endocrine lineage cells from the cell cycle, initially inducing cellular quiescence. Cellular senescence sets in as the exit from cell cycle becomes irreversible.

The polycomb gene *Bmi1* (4) is also involved in cell cycle exit during mouse endocrine cell lineage development. Proliferating β -cells from young mice express high levels of *Bmi1*, and low levels of *Cdkn2a/p16^{INK4}* (5–7). As mice age, BMI1 is displaced from the *p16^{INK4}* locus, resulting in increased *p16^{INK4}* expression and the consequent withdrawal of proliferating β -cells from the cell cycle. Similarly, β -cells in *Bmi1*-null mice

This work was supported by National Institutes of Health NIDDK Grants DK083762 and DK41301, and NIAID Grant U01DK085535. The authors declare that they have no conflicts of interest with the contents of this article. The content is solely the responsibility of the authors and does not necessarily represent the official views of the National Institutes of Health.

This article contains Figs. S1–S3 and Tables S1–S3.

¹ To whom correspondence should be addressed. Tel.: 310-794-5532; Fax: 310-206-0855; E-mail: mmartin@mednet.ucla.edu.

² The abbreviations used are: HLH, helix-loop-helix; bHLH, basic helix-loop-helix; BMI1, BMI1 proto-oncogene polycomb ring finger; CDK, cyclin-dependent kinase; CHGA, chromogranin A; cNEUROG1, cNEUROG3, and cCONTROL, constitutively expressing lentiviruses; Cum, cumate; Dox, doxycycline; GAST, gastrin; GIE, gastrointestinal endocrine; HES, hair/enhancer of split; MTT, 3-(4,5-dimethylthiazolyl-2)-2,5-diphenyltetrazolium bromide; NEUROD1, neurogenic differentiation factor 1; NEUROG3, neurogenin-3; NLS, nuclear localization signal; p16^{INK4a}, Cdkn2a cyclin-dependent kinase inhibitor 2a; p21^{CIP1}, Cdkn1a cyclin-dependent kinase inhibitor 1a; p27^{KIP1}, Cdkn1b cyclin-dependent kinase inhibitor 1b; p57^{KIP2}, Cdkn1c cyclin-dependent kinase inhibitor 1c; PCSK1, proprotein convertase subtilisin/kexin type 1; PTEN, phosphatase and tensin homolog; qPCR, quantitative PCR; SA- β -Gal, senescence-associated β -galactosidase; ANOVA, analysis of variance; PFA, paraformaldehyde.

become quiescent prematurely, reducing β -cell numbers with consequent failure of glucose homeostasis (5–7).

The role of *BMI1* as a mediator of senescence and quiescence is further highlighted by the recent observation that the population of *Bmi1*⁺ cells in the mouse intestinal crypt is enriched with quiescent early GIE lineage cells (8), likely related to *Neurog3*-expressing cells known to be concentrated in the same crypt domain (2). Since *Neurog3* expression is weak in the *Bmi1*⁺ population (8), *Bmi1* expression is likely downstream of *Neurog3*. Similar quiescent cells, identified by *mTert* expression, respond to post-fasting refeeding by repressing *Phosphatase and tensin homolog (Pten)* expression, and re-entering the cell cycle (9). These observations suggest that in mice, *Neurog3*'s cell cycle effects occur in early GIE lineage cells and are mediated downstream by *Bmi1* and *Pten*.

The phenotype of loss of *NEUROG3* function is similar in humans and mice, however, there are clinically significant differences. Notably, whereas loss of *NEUROG3* function in both humans and mice abolishes production of intestinal endocrine cells, β -cell development is less impacted in humans than in mice at birth, but results in severe diabetes in early childhood (10, 11). Therefore, it is of interest to establish whether *NEUROG3* expression in human pre-endocrine cells similarly induces exit from the cell cycle, and if so identify the mechanisms involved.

Here, we introduce the use of the BON4 cell line as a model for investigating the response of the human endocrine cell lineage to *NEUROG3*. We report that *NEUROG3* initially induces quiescence in a *p21*^{CIP1}-dependent manner. Furthermore, if *NEUROG3* expression is prolonged, then the initially reversible cycle arrest (cellular quiescence) gradually becomes permanent (cellular senescence). The early *NEUROG3*-induced cellular quiescence is reversible by inhibition of *PTEN*, due to reduction in steady-state *NEUROG3* levels in BON4 cells and human enteroids. We also report that the onset of *NEUROG3*-induced senescence is slowed due to concomitant induction of *BMI1* expression, which acts by attenuating *p16*^{INK4} expression.

Results

NEUROG3 inhibits the cell cycle in an endocrine cell line, but NEUROG1 does not

BON cells are a well-characterized human endocrine lineage cell line (12), from which a homogenous appearing BON4 subline was isolated; it expresses very low levels of *NEUROG3* and *NEUROG1* (Fig. S1, A and B). BON4 cells are readily transduced with constitutively active lentiviruses-encoding *NEUROG3* (c*NEUROG3*), *NEUROG1* (c*NEUROG1*), or Control sequence (cControl); expression is detectable within 1 day of transduction (Fig. S1, A and B). *NEUROG1* is a close proneural homolog of *NEUROG3*, not involved in GIE specification (13). In an unrelated study,³ to be published separately, we confirmed that the c*NEUROG3* lentivirus drives levels of *NEUROG3* expression similar to that seen in untransduced primary cultures of human intestinal epithelium undergoing active endocrine cell production.

Cumate (Cum)-inducible cell lines, denoted *BON4*_{Cum→*NEUROG3*}, *BON4*_{Cum→*NEUROG1*}, and *BON4*_{Cum→Control} were generated by transducing BON4 cells with Cum-inducible lentiviruses encoding *NEUROG3*, *NEUROG1*, or a Control sequence, respectively. Expression and protein were detectable within 1 day of adding Cum to the culture medium (Fig. S1, B and E).

We were unable to establish similar cell lines from BON4 cells successfully transduced with c*NEUROG3* because the cells quickly ceased proliferating, as assessed by the MTT assay (Fig. 1A), and loss of expression of the active cell cycle marker Ki67 (Fig. 1B, Fig. S1C). Analysis of the DNA content of the transduced cells by flow cytometry confirmed that the majority were in G₀-phase of the cell cycle, confirming that the cells exited the cell cycle (Fig. 1C). In contrast, control cells transduced with c*NEUROG1* proliferated actively and were indistinguishable from those transduced with control lentivirus (cControl) (Fig. 1, A–C).

The nuclear localization signal was deleted from the c*NEUROG3* construct (c*NEUROG3*: Δ NLS), to test the effect of reducing *NEUROG3* translocation to the nucleus. MTT assays show that c*NEUROG3*: Δ NLS has a largely impaired ability to induce cell cycle exit (Fig. S1D). These results demonstrate that *NEUROG3*, but not *NEUROG1*, induces human endocrine lineage cells to exit the cell cycle, via mechanisms requiring translocation to the nucleus.

NEUROG3 inhibits the cell cycle in most nonendocrine cell lines, but NEUROG1 does not

We also found that transduction with c*NEUROG3* induces cell cycle exit in cell lines derived from mesodermal tissues (macrophages, fibroblasts, and kidney) or endodermal tissues (stomach, colon, liver, and insulinoma), but transduction with c*NEUROG1* had no effect (Fig. 1D).

NEUROG1 was previously reported to induce cell cycle arrest in P19 cells, a mouse teratoma cell line with a well-characterized ability to differentiate into neural cells (14). We confirm that P19 cells exit the cell cycle when transduced with c*NEUROG1*, whereas c*NEUROG3* and cControl transduced cells were unaffected. Furthermore, a Cum-inducible *P19*_{Cum→*NEUROG1*} cell line was produced and responded to Cum induction by exiting the cell cycle, whereas a *P19*_{Cum→*NEUROG3*} cell line did not (Fig. 1, E and F).

NEUROG3 induces the expression of various mature GIE cell lineage markers in BON4 cells

Transduction of BON4 cells with c*NEUROG3* induces both protein and transcript expression of common GIE cell markers including chromogranin A (*CHGA*), proprotein convertase subtilisin/kexin type 1 (*PCSK1*), gastrin (*GAST*), and somatostatin (*SST*) (Fig. 2, A and B). Thus, *NEUROG3* not only induces cell cycle exit, but it also drives GIE cell differentiation.

NEUROG3-induced cell cycle arrest is p21^{CIP1}*-dependent*

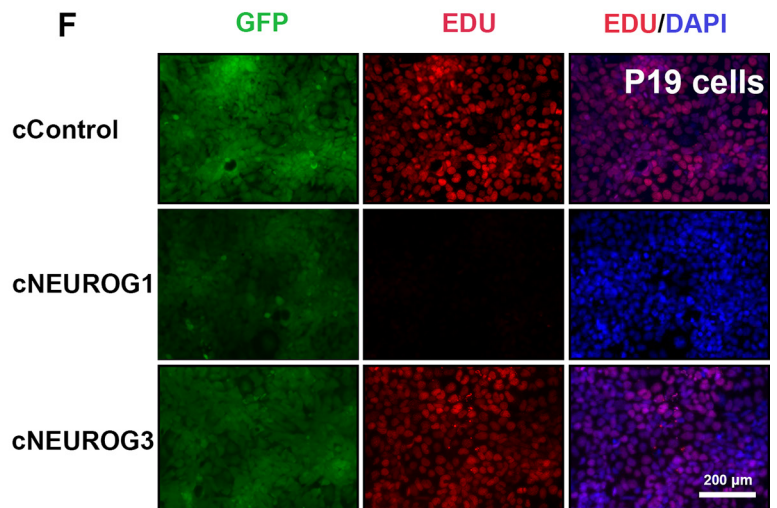
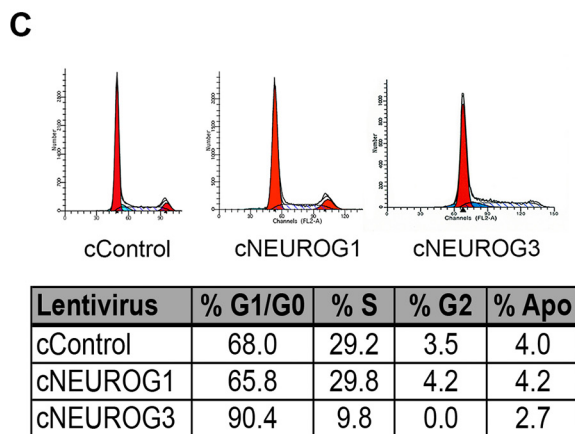
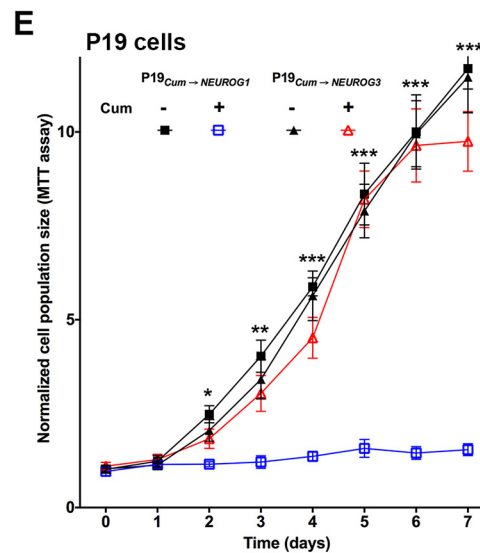
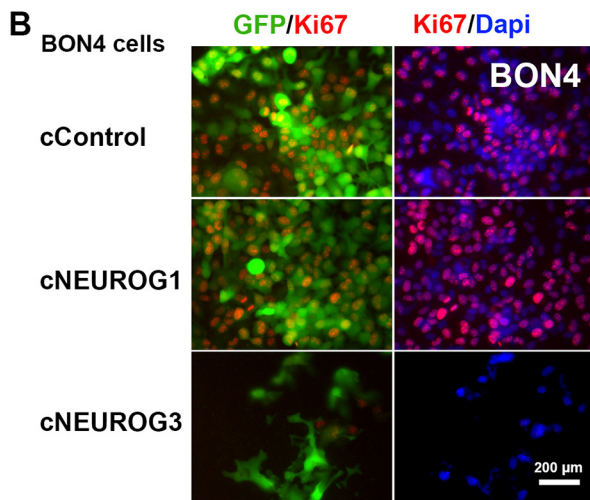
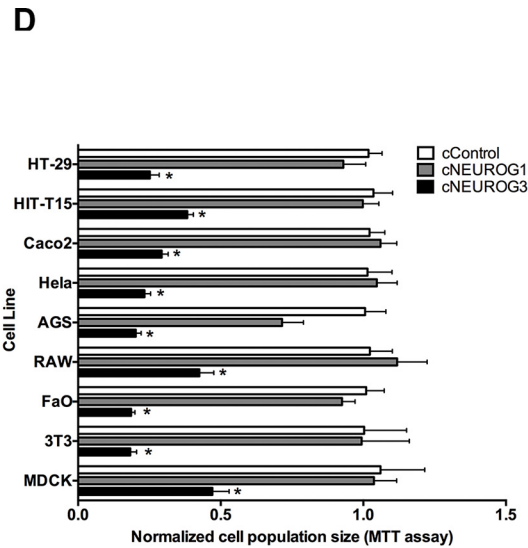
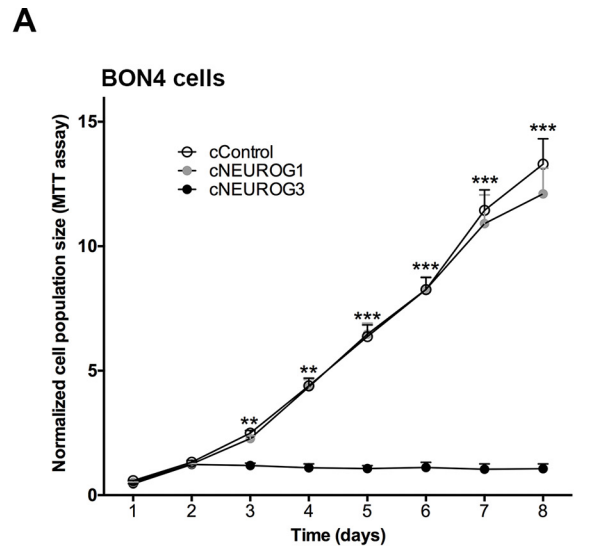
Changes in the expression of cyclin-dependent kinase inhibitors during *NEUROG3*-induced cell cycle exit were measured. *CDKN1A/p21*^{CIP1} and *CDKN1C/p57*^{KIP2} expression increased dramatically by day 1, and *CDKN2A/p16*^{INK4a} increased

³ R. S. Solorzano-Vargas, M. Bjerknes, J. Wang, S. V. Wu, M. G. Garcia-Careaga, D. Pisit, H. Cheng, M. S. German, S. Georgia, and M. G. Martín, unpublished data.

PTEN/BMI1 and NEUROG3 cellular arrest

steadily post-transduction, whereas *CDKN1B/p27^{KIP1}* expression was essentially constant following transduction of BON4 cells with cNEUROG3 (Fig. 3A).

We transduced *BON4_{Cum}→NEUROG3* cells with a doxycycline (Dox)-inducible *p21^{CIP1}* shRNA lentivirus, establishing a *BON4^{Dox}→shRNA(p21^{CIP1})_{Cum}→NEUROG3* doubly inducible cell line, which



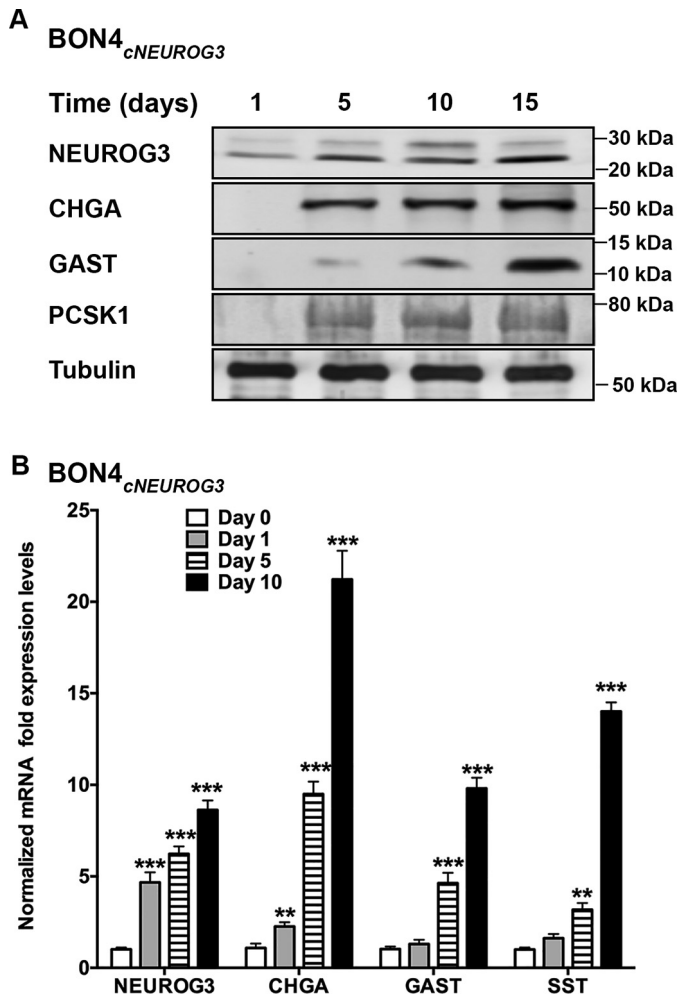


Figure 2. NEUROG3 induces several endocrine markers in BON4 cells. A, Western blotting of cells transduced with cNEUROG3 and assessed at various days for expression levels of NEUROG3-FLAG and several endocrine targets, including CHGA, GAST, and PCSK1. Western blots were performed 3 times and the figure is representative. B, qPCR assessment of endocrine transcripts over time following transduction with cNEUROG3 and standardized by tubulin. qPCR was performed from RNA isolated from 3 different samples and run in triplicate for each sample. Statistics: B, two-way ANOVA and two-way Tukey's multiple comparisons with adjusted *p* values.

we used to assess whether p21^{CIP1} is required for NEUROG3-induced cell cycle arrest. Dox induction of the shRNA decreased the p21^{CIP1} transcript level by 90% (Fig. 3, B, inset, and C). A control cell line, *BON4*^{Dox→shRNA(Control)}_{Cum→NEUROG3}, transduced with a Dox-inducible control shRNA was also generated.

The *BON4*^{Dox→shRNA(p21^{CIP1})}_{Cum→NEUROG3} and *BON4*^{Dox→shRNA(Control)}_{Cum→NEUROG3} cells proliferated normally in the absence of Cum or Dox. However, proliferation in both lines was strongly repressed upon

addition of Cum to the culture medium, due to the induction of NEUROG3 expression (Fig. 3B). In the absence of Cum, proliferation of *BON4*^{Dox→shRNA(p21^{CIP1})}_{Cum→NEUROG3} cells were not impacted by depleting p21^{CIP1} by adding Dox to the medium (Fig. 3B). Importantly, blocking p21^{CIP1} expression by adding Dox to the medium 3 days before inducing NEUROG3, strongly attenuated the cell cycle arrest and expression of endocrine differentiation markers induced by NEUROG3 (Fig. 3, B and C).

The rate of NEUROG3 degradation is increased if it is phosphorylated by cyclin-dependent kinases (CDKs) (15, 16). Depletion of p21^{CIP1}, a CDK inhibitor, could thereby lead to reduced NEUROG3 protein levels. Indeed, treatment of Cum-induced *BON4*^{Dox→shRNA(p21^{CIP1})}_{Cum→NEUROG3} cells with Dox results in a dramatic reduction in steady-state levels of NEUROG3 (Fig. 3D). However, depletion of p21^{CIP1} expression in control *BON4*^{Dox→shRNA(p21^{CIP1})}_{Cum→NEUROG1} cells had no effect on proliferation and NEUROG1 levels (Fig. 3D, data not shown).

Finally, we confirmed that NEUROG3, but not NEUROG1, directly interacts with E box elements within the immediate promoter region of p21^{CIP1}. Direct functional interaction of NEUROG3 with the human p21^{CIP1} promoter was demonstrated using a luciferase expression reporter assay (Fig. S1F), and a chromatin immunoprecipitation (ChIP) assay of BON4 cells expressing FLAG-tagged NEUROG3 (Fig. S1G). These findings demonstrate that NEUROG3-induced cell cycle exit is mediated by direct interaction with the p21^{CIP1} promoter.

NEUROD1 expression is not required for NEUROG3-induced quiescence

The bHLH transcription factor NEUROD1 is a major downstream NEUROG3 target (17), so we assessed its role in NEUROG3-induced quiescence. NEUROD1 protein is readily detectable in BON4 cells, and its expression increased following transduction with cNEUROG3, but not following cNEUROG1 transduction (Fig. S2A). We transduced *BON4*_{Cum→NEUROG3} cells with a Dox-inducible NEUROD1 shRNA lentivirus, establishing a *BON4*^{Dox→shRNA(NEUROD1)}_{Cum→NEUROG3} doubly inducible cell line. Dox induction of shRNA expression significantly decreased NEUROD1 mRNA and protein levels (Fig. S2B). Importantly, the NEUROG3-induced cell cycle exit was not rescued by blocking the NEUROG3-induced up-regulation of NEUROD1 (Fig. S2C); therefore, NEUROD1 up-regulation is not required for the NEUROG3-induced cell cycle exit.

Actively proliferating BON4 cells express NEUROD1; therefore, it is noteworthy that proliferation continues, but at a significantly slower pace, following NEUROD1 knockdown by Dox-treating *BON4*^{Dox→shRNA(NEUROD1)}_{Cum→NEUROG3} cells (Fig. S2C). This

Figure 1. NEUROG3 induces cell cycle arrest. A, MTT analysis of BON4 cells transduced with constitutive cNEUROG3, cNEUROG1, or cControl lentiviruses assessed daily at the indicated time points after transduction. The experiment was performed on three separate occasions and each by triplicate. B, representative images of Ki67 and 4',6-diamidino-2-phenylindole (Dapi) staining of cells transduced 5 days earlier with lentiviruses. Staining was performed in 6 different assays, and images are representative. C, FACS analysis was performed on day 5 of cells transduced with the various lentiviruses. Shown are a representative histogram and result of three separate experiments performed in triplicate. D, cNEUROG3, cNEUROG1, or cControl lentiviruses were transduced into the indicated cells lines, and the MTT assay assessed 5 days later. E, MTT analysis of Cum or vehicle-treated *P19*_{Cum→NEUROG3} and *P19*_{Cum→NEUROG1} cells assessed daily at the indicated time points. F, Edu-treated *P19*_{Cum→NEUROG3} and *P19*_{Cum→NEUROG1} cells following Cum treatment for 5 days and incubated with 1 μM Edu for 24 h. Three separate experiments were performed in triplicate, and the graph represents the data from the three experiments. Statistics: A, D, and E: two-way ANOVA and two-way Tukey's multiple comparisons with adjusted *p* values.

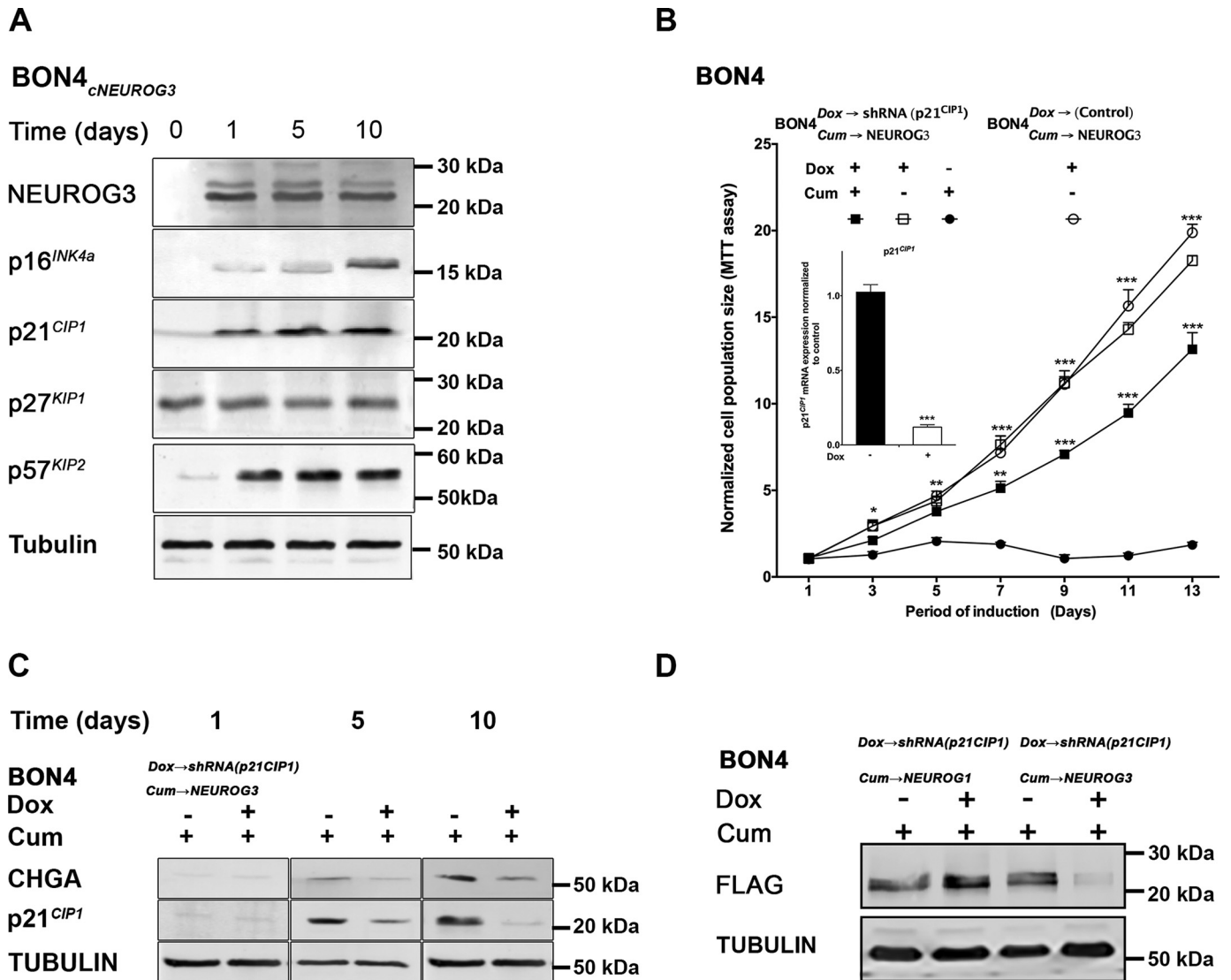


Figure 3. NEUROG3 induces several cell cycle inhibitors in BON4 cells. *A*, time course of cells transduced with cNEUROG3 lentivirus and assessed by Western blot analysis over several days. *B*, $BON4^{Dox \rightarrow shRNA(p21^{CIP1})}_{Cum \rightarrow NEUROG3}$ cells were treated with and without Cum and/or Dox, and $BON4^{Dox \rightarrow Control}_{Cum \rightarrow NEUROG3}$ cells were treated with Dox, and processed every other day for 13 days and a MTT assay was performed at different time points. *Inset*, p21 mRNA levels with or without Dox at day 3. *C*, $BON4^{Dox \rightarrow shRNA(p21^{CIP1})}_{Cum \rightarrow NEUROG3}$ cells treated with Cum with or without Dox, and Western blot analysis performed at various time points using anti-CHGA, p21, and tubulin. *D*, Western blotting of $BON4^{Dox \rightarrow shRNA(p21^{CIP1})}_{Cum \rightarrow NEUROG1}$ and $BON4^{Dox \rightarrow shRNA(p21^{CIP1})}_{Cum \rightarrow NEUROG3}$ cells treated with Cum with or without Dox, and protein isolate was probed with anti-FLAG and tubulin Abs. Statistics: *B*, two-way ANOVA and two-way Tukey's multiple comparisons with adjusted *p* values.

observation indicates that baseline *NEUROD1* expression promotes BON4 cell proliferation.

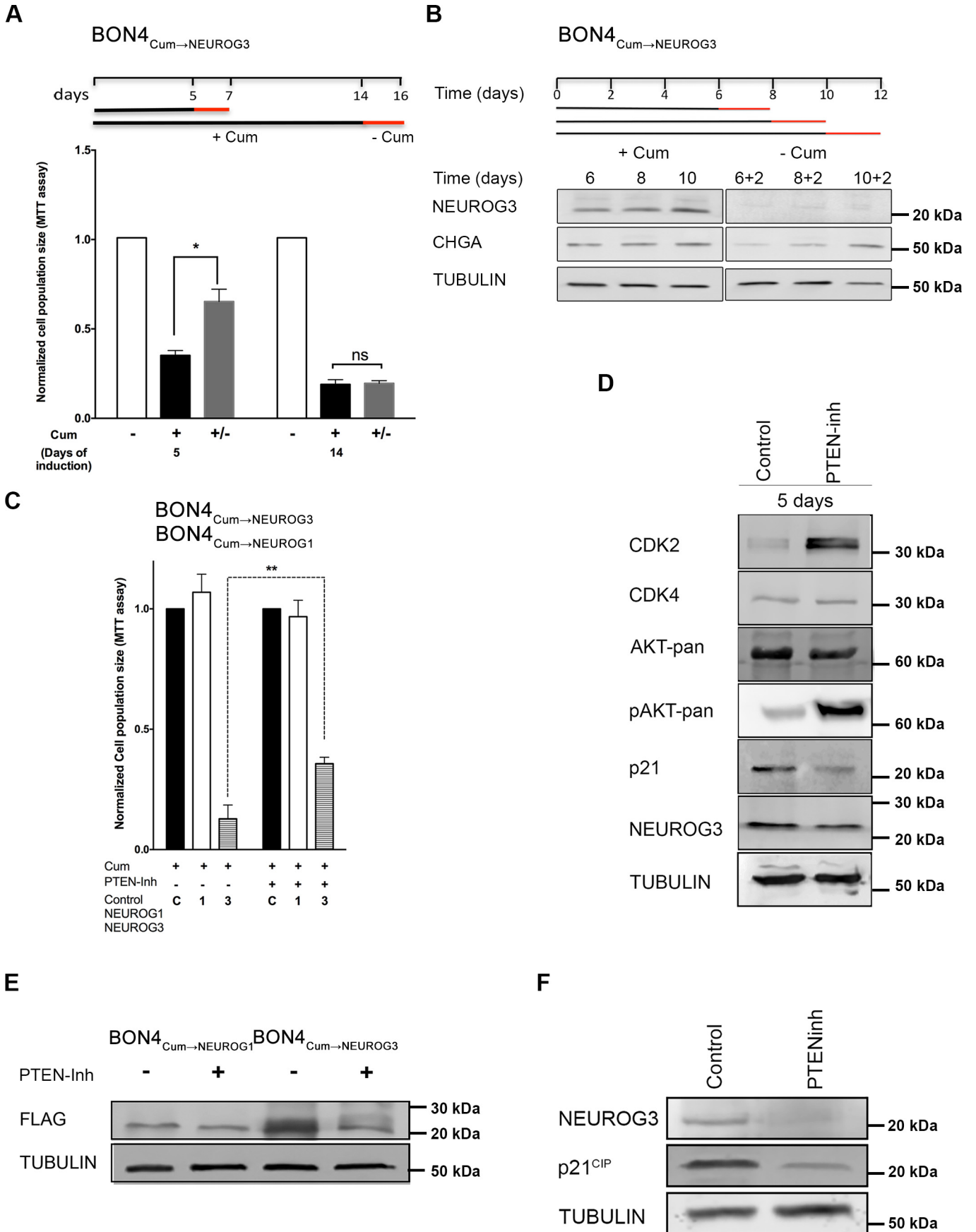
NEUROG3-induced cell cycle exit is initially reversible but becomes irreversible with time

$BON4_{Cum \rightarrow NEUROG3}$ cells undergoing various durations of Cum-induced cell cycle exit differ in the extent of their recovery 2 days after cessation of Cum treatment, by which time *NEUROG3* levels are significantly reduced (Fig. S1E, Fig. 4B). The cell cycle exit induced by short-term treatment (<6 days) was reversible, whereas long-term treatment (10 days) was not (Fig. 4A). Similarly, the induction of expression of the endocrine differentiation marker *CHGA* declined 2 days after a short-term (<6 days), but not after long-term treatment, suggesting that short-term exposure to *NEUROG3* is insufficient to “lock in” an endocrine cell fate (Fig. 4B).

PTEN inhibition reverses NEUROG3-induced quiescence, by decreasing NEUROG3 protein

The phosphatase PTEN has been implicated in the process of cell cycle re-entry by quiescent mouse intestinal cells (9). PTEN is ubiquitously expressed in human cells (18), prompting us to test if PTEN function is involved in *NEUROG3*-induced quiescence in human BON4 cells.

A *NEUROG3*-induced quiescent state was invoked by adding Cum to the culture medium of $BON4_{Cum \rightarrow NEUROG3}$. On day 3 of Cum treatment, bisperoxovanadium-pic (bpV(pic), a specific PTEN inhibitor (19); 100 nM final concentration), or an equal volume of vehicle in matched controls, was added to the culture medium. Control $BON4_{Cum \rightarrow NEUROG1}$ and $BON4_{Cum \rightarrow Control}$ cells underwent similar Cum and bpV(pic) treatments. Cell proliferation and *NEUROG3* protein levels were measured 1 day later.



PTEN/BMI1 and NEUROG3 cellular arrest

Quiescent Cum-treated $BON4_{Cum \rightarrow NEUROG3}$ cells had resumed proliferating after 1 day of PTEN inhibition, whereas vehicle-treated controls remained quiescent (Fig. 4C). Furthermore, PTEN inhibition activated phospho-AKT and CDK2 (Fig. 4D), whereas NEUROG3 and $p21^{CIP1}$ levels were significantly decreased, compared with vehicle-treated controls (Fig. 4E). In contrast, NEUROG1 levels in Cum-induced $BON4_{Cum \rightarrow NEUROG1}$ cells were unaffected by PTEN inhibition (Fig. 4E). Similarly, PTEN inhibition of human enteroids attenuated NEUROG3 and $p21^{CIP1}$ levels (Fig. 4F).

Prolonged NEUROG3 expression leads to cellular senescence in a $p21^{CIP1}$ -dependent manner

Prolonged exposure of $BON4_{Cum \rightarrow NEUROG3}$ cells to Cum gradually induces strong $p16^{INK4a}$ expression (Fig. 3A). Such cells fail to re-enter the cell cycle following Cum withdrawal (Fig. 4A), indicating that they have become senescent. To confirm their senescence, we stained a time series of such cells for senescence-associated β -Gal (SA- β -Gal), a marker of cellular senescence (20). SA- β -Gal activity was undetectable in $BON4_{Cum \rightarrow NEUROG3}$ cells during the first 5 days of Cum exposure (Fig. 5A) despite the detection of low and slowly increasing levels of $p16^{INK4a}$ expression at that time (Fig. 3A). However, SA- β -Gal activity was discernible after 6 days of Cum exposure, and by 8 days most cells were SA- β -Gal positive (Fig. 5A), confirming their senescence. Control $BON4_{Cum \rightarrow Control}$ and $BON4_{Cum \rightarrow NEUROG1}$ cells treated with Cum continued proliferating (Fig. 1A) and remained negative for SA- β -Gal (data not shown).

Robust expression of $p21^{CIP1}$ is necessary to institute NEUROG3-induced quiescence (Fig. 3, A and B), but it remains unclear whether prolonged NEUROG3 expression, in the absence of up-regulation of $p21^{CIP1}$, is sufficient on its own to eventually drive cells into quiescence and senescence. We tested this by the simultaneous exposure of $BON4_{Cum \rightarrow NEUROG3}^{Dox \rightarrow shRNA(p21^{CIP1})}$ cells to Cum and Dox, which prevented quiescence and senescence for as long as we tested (15 days). In contrast, $BON4_{Cum \rightarrow NEUROG3}^{Dox \rightarrow shRNA(p21^{CIP1})}$ Cum alone rapidly became quiescent and eventually senescent. This demonstrates that NEUROG3-induced quiescence and senescence requires $p21^{CIP1}$ (Fig. 5, B and C). It should be noted, however, that in the absence of $p21^{CIP1}$, the resultant Cum-induced NEUROG3 protein level is diminished (Fig. 3D), which may have weakened its impact.

For comparison, we examined the cell cycle state induced by treating $BON4_{Cum \rightarrow NEUROG3}^{Dox \rightarrow shRNA(NEUROD1)}$ cells with Dox, which represses baseline *NEUROD1* expression, greatly attenuating proliferation (Fig. S2, A–C). These cells remained in a slowly cycling quiescent state for a prolonged period without

becoming senescent, as indicated by their minimal growth and lack of SA- β -Gal staining even after 15 days (Fig. S2D). Thus, prolonged NEUROG3 exposure in the absence of $p21^{CIP1}$ -induced quiescence, or prolonged quiescence in the absence of NEUROG3-induced $p21^{CIP1}$ up-regulation, are both insufficient to induce senescence in BON4 cells.

NEUROG3 induces BMI1 expression, which attenuates the induction of $p16^{INK4a}$, delaying the onset of senescence

The polycomb group protein BMI1 is involved in regulating pancreatic β -cell senescence by repressing $p16^{INK4a}$ expression (see Introduction). This led us to suspect that BMI1 may similarly be involved in limiting $p16^{INK4a}$ expression in the early quiescent phase of NEUROG3 expression in BON4 cells (Fig. 3A), thereby delaying the onset of senescence. Indeed, Cum treatment of $BON4_{Cum \rightarrow NEUROG3}$ cells led to increased *BMI1* mRNA and protein levels within hours, whereas BMI1 did not change in Cum-treated control $BON4_{Cum \rightarrow NEUROG1}$ cells (Fig. 6A; Fig. S3A; data not shown). Direct functional interaction of NEUROG3 with the human *Bmi1* promoter was demonstrated using a luciferase expression reporter assay (Fig. 6B), and a ChIP assay of BON4 cells transfected with FLAG-tagged NEUROG3 (Fig. 6C) (21).

We assessed whether *Bmi1* impairs NEUROG3 binding to the E box in the $p21^{CIP1}$ promoter (22). We examined the loss of BMI1 function with specific *Bmi1* inhibitor PTC-209 (1.25 μ M). The addition of *Bmi1* inhibitor significantly enhanced NEUROG3 induction of the human $p21^{CIP1}$ promoter using a luciferase expression reporter assay (Fig. 6D), and by ChIP assay in BON4 cells (Fig. 6E).

The impact of loss of BMI1 in the context of NEUROG3-induced quiescence was determined by simultaneous treatment of $BON4_{Cum \rightarrow NEUROG3}$ cells with Cum and PTC-209. The cells exhibited a dramatic increase in expression of $p16^{INK4a}$, $p19^{INK4d}$, and *CHGA* expression (Fig. 6F), accompanied by an accelerated onset of cellular senescence as assessed by SA- β -Gal (Fig. 6G). In contrast, inhibition of BMI1 in cells not treated with Cum (and hence not up-regulating NEUROG3) did not undergo senescence. Taken together, these data indicate that within this *in vitro* system, short-term NEUROG3 induces $p21^{CIP1}$ and *BMI1* expression, the latter acting to attenuate the up-regulation of $p16^{INK4a}$ and $p19^{INK4d}$ levels, thereby delaying the onset of NEUROG3-induced cellular senescence.

Discussion

We have found that the human endocrine-derived BON4 cell line responds to the pro-endocrine transcription factor NEUROG3 by rapidly exiting the cell cycle and expressing markers of endocrine differentiation as outline in Fig. 6H.

Figure 4. NEUROG3 induces cellular quiescence and senescence in a time-dependent fashion. A, MTT assay of $BON4_{Cum \rightarrow NEUROG3}$ cells treated with either vehicle or Cum for 5 or 14 days and processed, whereas others were treated for a similar amount of time, and then Cum was removed for 2 days before processing. B, $BON4_{Cum \rightarrow NEUROG3}$ cells were treated with either vehicle or Cum for various times, whereas others were treated for a similar amount of time, and then Cum was removed for 2 days before processing. Cell extracts were assessed by Western blotting with anti-NEUROG3, CHGA, or tubulin. C, MTT assay of $BON4_{Cum \rightarrow NEUROG3}$, $BON4_{Cum \rightarrow NEUROG1}$, and $BON4_{Cum \rightarrow Control}$ cells treated with Cum for 5 days with or without the PTEN inhibitor, bpV(pic), at a concentration of 100 nM on the last day. D, Western blotting of BON4 cells transiently transfected with a NEUROG3 expressing vector 5 days earlier with or without bpV(pic). E, Western blotting of $BON4_{Cum \rightarrow NEUROG3}$, and $BON4_{Cum \rightarrow NEUROG1}$ cells treated with Cum for 3 days, and then with or without the PTEN inhibitor for 3 additional days. Blot was probed with anti-FLAG (to detect the C-terminal FLAG tag of *NEUROG3/NEUROG1*), anti- $p21^{CIP1}$, or anti-tubulin antibody. F, Western blotting of human enteroids treated with and without the PTEN inhibitor for 3 additional days. Statistics: C, two-way ANOVA and two-way Tukey's multiple comparisons with adjusted *p* values.

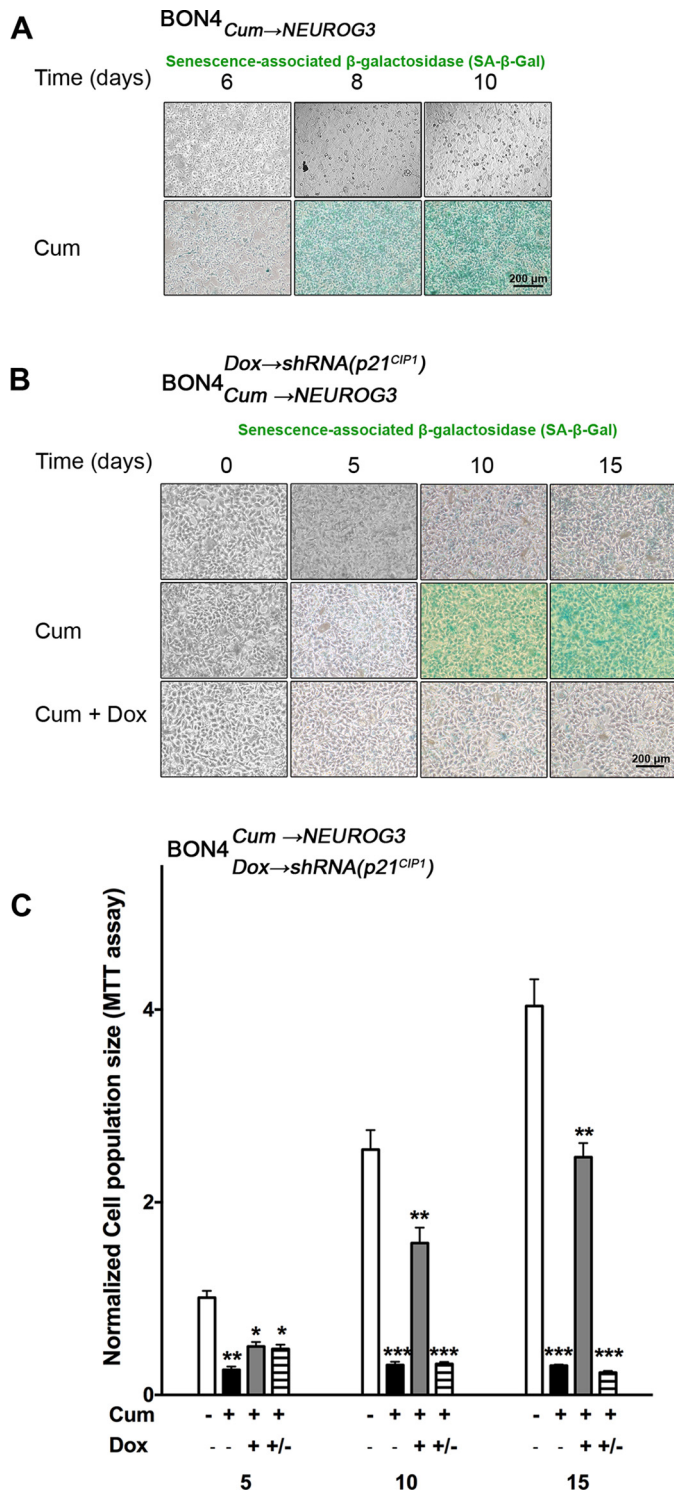


Figure 5. Prolong NEUROG3 expression induces cellular senescence. A, SA-β-Gal staining of BON4_{Cum→NEUROG3} cells treated with Cum or vehicle for either 6, 8, or 10 days. B, SA-β-Gal staining of BON4_{Dox→shRNA(p21^{CIP1})} Cum → NEUROG3 cells treated with or without Cum, Dox, or vehicle control for various lengths of time. C, MTT assay of BON4_{Dox→shRNA(p21^{CIP1})} Cum → NEUROG3 cells treated with or without Cum, Dox, or vehicle control as with A or B. Cells were also treated with Cum and Dox for specific lengths of time, and 2 days later Dox was removed (+/-). All experiments performed 3–4 times in triplicate and representative data presented. Statistics: C, two-way ANOVA and two-way Tukey’s multiple comparisons with adjusted *p* values.

Interestingly, we also found that NEUROG3 drives a similar cell cycle exit in a wide variety of cell lines, but that its homolog NEUROG1 does not. P19 cells is a singular exception. We found that NEUROG3 expression has little effect on P19 cells, whereas NEUROG1 stimulates p27^{KIP1} expression and induces cell cycle exit (Fig. 1, E and F, data not shown), consistent with the cell line’s neurogenic response to NEUROG1 (14). The failure of NEUROG3 to act in P19 cells, despite P19 cell’s well-characterized pluripotency, warrants future investigation.

We also found that if p21^{CIP1} expression is repressed, then NEUROG3 fails to induce BON4 cell quiescence and endocrine differentiation (Fig. 3, B and C), as others have shown in mouse pancreas (3, 23). This dependence of NEUROG3 on p21^{CIP1} is due to the direct action of NEUROG3 at the p21^{CIP1} promoter (Fig. S1, F and G), explaining why deleting the nuclear localization signal impairs NEUROG3’s ability to induce cell cycle arrest (Fig. S1D).

Phosphorylation of NEUROG3 has recently been shown to increase its degradation (15, 16). This explains our observation that NEUROG3 protein levels were diminished after p21^{CIP1} repression (Fig. 3D) or PTEN inhibition (Fig. 4, E and F), both of which regulate protein phosphorylation (24–26).

In mouse pancreas, newly differentiating endocrine cells require a short burst of high levels of NEUROG3 exposure to induce differentiation, whereas adult mouse β-cells require tonic low levels of NEUROG3 expression to sustain hormone production (27). We have similarly found that transient NEUROG3 expression in BON4 cells induces cellular quiescence and commencement of endocrine differentiation, both of which are reversible if NEUROG3 is reduced (either by removing Cum-induction, or via increased NEUROG3 phosphorylation and consequent degradation following p21^{CIP1} or PTEN inhibition). Prolonged expression of NEUROG3 results in senescence and sustained endocrine differentiation.

In BON4 cells, NEUROG3 also drives BMI1 expression, which in turn acts to delay senescence by constraining NEUROG3-induced expression of p21^{CIP1} and p16^{INK4a} (Fig. 6, A–F and H). Chemical inhibition of BMI1 function accelerates the NEUROG3-induced expression of p16^{INK4a}, p19^{ARF}, endocrine differentiation, and senescence (Fig. 6F). This may explain the pancreatic endocrine maturation strategy, intense short bursts induce cell cycle exit, initiates differentiation, and increases BMI1 expression, which acts to restrain premature p16 expression, facilitating cell cycle re-entry during the post-natal islet growth, and remodeling. As β-cells mature, low-grade expression of NEUROG3 reinforces the endocrine program, but the resultant low BMI1 and high p16 levels render β-cells more refractory to cell cycle re-entry.

It is important to note that whereas the BON4 cell line provides a tractable model in which to explore the consequences of a NEUROG3-induced endocrine state in human cells, its use has caveats. The parental BON cell line was generated from a metastatic human carcinoid tumor of pancreas (12), and hence displays abnormalities including continuous proliferation and high basal levels of hair/enhancer of split-1 (*HES1*) and *NEUROD1* expression (Fig. S2A, data not shown). *Hes1* is a direct target of Notch and is a potent transcriptional inhibitor

PTEN/BMI1 and NEUROG3 cellular arrest

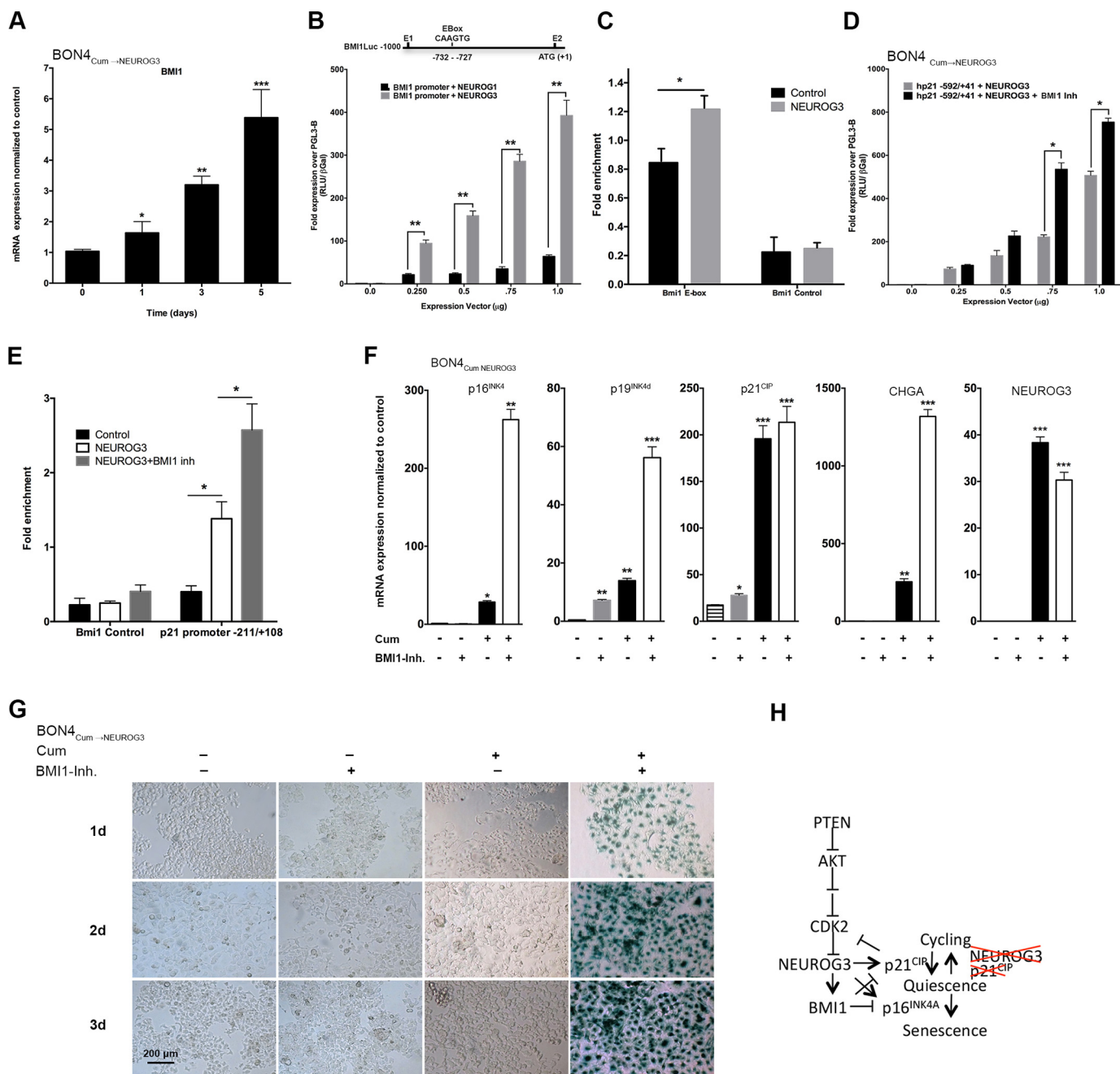


Figure 6. NEUROG3 induces BMI1 expression, which attenuates p16, p19, and the GIE phenotype. *A*, Western blotting of $BON4_{Cum \rightarrow NEUROG3}$ cells stimulated with Cum for 5 days in the presence or absence of BMI1 inhibitors for up to 2 days and assessed for BMI1 and tubulin. *B*, cells transiently transfected with human BMI1 promoter (-100/+1) luciferase construct, and with various amounts of either NEUROG3 or NEUROG1 pGL3-basic expressing vector, and luciferase were measured and normalized with β -Gal after 3 days. *C*, ChIP assay for NEUROG3-FLAG binding to E-box elements in the BMI1 promoter. *D*, cells transiently transfected with human p21 promoter (-592/+41) and various amounts of NEUROG3 pGL3-basic expressing vector with and without BMI1 inhibitor for the last 24 h and luciferase were measured and normalized with β -Gal after 3 days. *E*, ChIP assay for NEUROG3-FLAG binding to E-box elements in the p21 promoter of cells transfected with NEUROG3 and treated with and without Bmi1inh. *F*, quantitative PCR assessments of CHGA, NEUROG3, p16, p19, and p21 were performed from total RNA of $BON4_{Cum \rightarrow NEUROG3}$ cells treated with or without Cum for 3 days and BMI1 inhibitor for 3 days. *G*, SA- β Gal staining assay of $BON4_{Cum \rightarrow NEUROG3}$ cells treated with or without Cum in the presence or absence of BMI1 inhibitor. All experiments were performed 3–4 times in triplicate and representative data are presented. *H*, proposed model of PTEN and BMI1 modulation NEUROG3 effects on the cell cycle. Statistics: *A–D*, one-way ANOVA and Dunnett's multiple comparison and adjusted *p* values; *E* and *F*, two-way ANOVA and two-way Tukey's multiple comparisons with adjusted *p* values.

of bHLH transcription factors, as well as CDK inhibitors (28, 29). Therefore, it is plausible that the high basal levels of HES1 in BON4 cells represses endogenous expression of NEUROG3 and the CIP/KIP genes. Robust HES1 expression in BON4 cells would be expected to inhibit NEUROD1 expression; but in fact, NEUROD1 is surprisingly abundant in these cells, and as we have shown here, is required to drive their baseline prolifera-

tion. In contrast, NEUROD1 is known to induce cell cycle arrest when expressed in various cell lines or in secretin-expressing GIE cells (30). Interestingly, we also found that BON4 cells express high levels of RFX6 mRNA, a transcription factor that functions both up- and downstream of NEUROG3 (data not shown). Although not assessed here, RFX6 may have a role in driving NEUROD1 expression in the absence of NEUROG3 (31).

Experimental procedures

Statistics

The data throughout the manuscript are presented as the mean \pm S.E. Multiple *t* tests were performed using GraphPad Prism software, and significant *p* values (*, <0.01; **, <0.001; ***, <0.0001) are indicated in all the figures.

Antibodies, oligonucleotides, and vectors

The various antibodies, primers used for quantitative PCR (qPCR), vectors and viruses used are listed in Tables S1–S3. Oligonucleotides used for ChIP, and site-directed mutagenesis will be made available upon request.

Cell lines

Most established cell lines were obtained from ATCC and propagated and maintained as suggested. The BON4 cell line used in this study was generated from the BON cell line, obtained from Dr. Townsend (University of Texas Medical Branch, Galveston, TX). The parental BON that had a more heterogeneous appearance and growth characteristics were maintained in Dulbecco's modified Eagle's medium/F-12 media supplemented with 10% FBS (12).

Lentiviral development and transduction

The single exon *NEUROG1* was PCR amplified from human genomic DNA with a C-terminal FLAG tag oligonucleotide. Sequence encoding a C-terminal FLAG tag was also added to a previously described human *NEUROG3* cDNA and along with *NEUROG1* the constructs were cloned into a lentivirus-based vector to generate constitutively active lentivirus (10). To generate the *NEUROG1*- and *NEUROG3*-inducible lentiviruses, both were subcloned into SparQ-IRES-GFP lentivector. Attenuation of various transcripts was performed using lentiviral shRNA that were purchased from a commercial vendor and are displayed in Table S3. Cells' containing an inducible system were supplemented with either Cum (30 μ g/ml) or Dox (1 μ g/ml) and replaced every other day.

Cell proliferation analysis by MTT and FACS

Cell proliferation was assessed by standard MTT assay (32). By FACS analysis, cells were harvested and fixed with 4% PFA. After fixation, cells were resuspended in PBS containing propidium iodine and RNase A, and analyzed for DNA content by flow cytometry using ModFitLt V3 (pMAC). Data are representative of at least 3 separate experiments performed in triplicate.

Luciferase reporter assay

Luciferase assay was performed as previously described (10). Various constructs were transfected using Lipofectamine, and lysates were used to measure luciferase that was normalized by *Renilla* luciferase.

Western blot analysis

Cells were lysed and 10 μ g of protein was loaded onto a 10% polyacrylamide gel and subjected to SDS-PAGE before blotting onto an immune blot from Amersham Biosciences, Hybond. Membranes were blotted using standard procedures using the

antibodies shown in Table S1. Western blots were visualized using the ECL plus Western blotting kit and scanned on an imager.

qPCR

qPCR with cDNA synthesized from 5 μ g of total RNA was performed either with TaqMan assay, or using Perfecta SYBR[®] Green SuperMix, Low ROX[™] in a real-time Thermocycler. The results obtained for each individual gene were normalized to β -tubulin expression in the sample. The primers used were designed with Primer3, or as suggested by TaqMan, and are shown in Table S2.

SA- β -Gal staining

SA- β -Gal staining was used to determine replicative senescence (33). Cells were washed with PBS and fixed with 4% PFA, and SA- β -Gal staining solution was incubated, and observed every 4 h for 12 h, and then every 12 h. The optimal incubation period was determined based on the visibility of stained cells in the test sample, but not in the control sample.

Chromatin immunoprecipitation (ChIP)

ChIP experiments were carried out using modifications to the micro-ChIP protocol (34). Briefly, BON4 cells were treated with 1% PFA to cross-link the DNA with bound proteins. After washing, the cells were lysed in SDS-based lysis buffer with protease inhibitors, sonicated to shear chromatin to an average size of 500 bp, and cellular debris was removed by centrifugation. Anti-FLAG-M2 antibody was bound to protein G-coated magnetic beads, and diluted chromatin lysate was incubated overnight with antibody-bound magnetic beads and washed in RIPA buffer and TE. Cross-links were reversed and the DNA was purified and quantified by qPCR using SYBR Green PCR. DNA enrichment data were estimated as the percentage bound/input ratio, presented relative to the un-induced control.

Immunofluorescent staining

BON4 cells transduced with one of several lentiviruses and were grown on glass coverslips and subsequently fixed in 4% PFA and washed with PBS before treating with blocking buffer and incubating with primary and secondary antibodies listed in Tables S1–S3.

Statistics

For all other multiple comparisons, one-, or two-way ANOVA was followed by Tukey's or Dunnett's multiple comparisons test. For comparisons involving one independent variable with two groups, we performed Student's *t* tests. Statistical significance was set at: *, *p* < 0.05; **, 0.01; and ***, 0.005, with respect to final (adjusted) *p* values. Variation is reported as S.E.

Author contributions—R. S. S.-V. and M. G. M. conceptualization; R. S. S.-V., M. B., and M. G. M. data curation; R. S. S.-V., M. B., S. V. W., S. G., and M. G. M. formal analysis; R. S. S.-V., J. W., S. D., H. C., and M. G. M. investigation; M. B., H. C., S. G., and M. G. M. writing-original draft; M. B., S. G., and M. G. M. writing-review and editing; M. S., J. C. D., and M. G. M. funding acquisition; M. G. M. project administration.

References

1. Gu, G., Dubauskaite, J., and Melton, D. A. (2002) Direct evidence for the pancreatic lineage: NGN3⁺ cells are islet progenitors and are distinct from duct progenitors. *Development* **129**, 2447–2457 [CrossRef Medline](#)
2. Bjerknes, M., and Cheng, H. (2006) Neurogenin 3 and the enteroendocrine cell lineage in the adult mouse small intestinal epithelium. *Dev. Biol.* **300**, 722–735 [CrossRef Medline](#)
3. Miyatsuka, T., Kosaka, Y., Kim, H., and German, M. S. (2011) Neurogenin3 inhibits proliferation in endocrine progenitors by inducing Cdkn1a. *Proc. Natl. Acad. Sci. U.S.A.* **108**, 185–190 [CrossRef Medline](#)
4. Alkema, M. J., Bronk, M., Verhoeven, E., Otte, A., van 't Veer, L. J., Berns, A., and van Lohuizen, M. (1997) Identification of Bmi1-interacting proteins as constituents of a multimeric mammalian polycomb complex. *Genes Dev.* **11**, 226–240 [CrossRef Medline](#)
5. Tschen, S. I., Georgia, S., Dhawan, S., and Bhushan, A. (2011) Skp2 is required for incretin hormone-mediated beta-cell proliferation. *Mol. Endocrinol.* **25**, 2134–2143 [CrossRef Medline](#)
6. Tschen, S. I., Dhawan, S., Gurlo, T., and Bhushan, A. (2009) Age-dependent decline in beta-cell proliferation restricts the capacity of beta-cell regeneration in mice. *Diabetes* **58**, 1312–1320 [CrossRef Medline](#)
7. Dhawan, S., Tschen, S. I., and Bhushan, A. (2009) Bmi-1 regulates the Ink4a/Arf locus to control pancreatic beta-cell proliferation. *Genes Dev.* **23**, 906–911 [CrossRef Medline](#)
8. Yan, K. S., Gevaert, O., Zheng, G. X. Y., Anchang, B., Probert, C. S., Larkin, K. A., Davies, P. S., Cheng, Z. F., Kaddis, J. S., Han, A., Roelf, K., Calderon, R. I., Cynn, E., Hu, X., Mandleywala, K., *et al.* (2017) Intestinal enteroendocrine lineage cells possess homeostatic and injury-inducible stem cell activity. *Cell Stem Cell* **21**, 78–90.e76 [CrossRef Medline](#)
9. Richmond, C. A., Shah, M. S., Deary, L. T., Trotter, D. C., Thomas, H., Ambruzs, D. M., Jiang, L., Whiles, B. B., Rickner, H. D., Montgomery, R. K., Tovaglieri, A., Carlone, D. L., and Breault, D. T. (2015) Dormant intestinal stem cells are regulated by PTEN and nutritional status. *Cell Rep.* **13**, 2403–2411 [CrossRef Medline](#)
10. Wang, J., Cortina, G., Wu, S. V., Tran, R., Cho, J. H., Tsai, M. J., Bailey, T. J., Jamrich, M., Ament, M. E., Treem, W. R., Hill, I. D., Vargas, J. H., Gershman, G., Farmer, D. G., Reyen, L., and Martín, M. G. (2006) Mutant neurogenin-3 in congenital malabsorptive diarrhea. *N. Engl. J. Med.* **355**, 270–280 [CrossRef Medline](#)
11. Pauerstein, P. T., Sugiyama, T., Stanley, S. E., McLean, G. W., Wang, J., Martín, M. G., and Kim, S. K. (2015) Dissecting human gene functions regulating islet development with targeted gene transduction. *Diabetes* **64**, 3037–3049 [CrossRef Medline](#)
12. Evers, B. M., Townsend, C. M., Jr., Upp, J. R., Allen, E., Hurlbut, S. C., Kim, S. W., Rajaraman, S., Singh, P., Reubi, J. C., and Thompson, J. C. (1991) Establishment and characterization of a human carcinoid in nude mice and effect of various agents on tumor growth. *Gastroenterology* **101**, 303–311 [CrossRef Medline](#)
13. Zou, D., Silvius, D., Fritsch, B., and Xu, P. X. (2004) Eya1 and Six1 are essential for early steps of sensory neurogenesis in mammalian cranial placodes. *Development* **131**, 5561–5572 [CrossRef Medline](#)
14. Farah, M. H., Olson, J. M., Sucic, H. B., Hume, R. I., Tapscott, S. J., and Turner, D. L. (2000) Generation of neurons by transient expression of neural bHLH proteins in mammalian cells. *Development* **127**, 693–702 [Medline](#)
15. Krentz, N. A. J., van Hoof, D., Li, Z., Watanabe, A., Tang, M., Nian, C., German, M. S., and Lynn, F. C. (2017) Phosphorylation of NEUROG3 links endocrine differentiation to the cell cycle in pancreatic progenitors. *Dev. Cell* **41**, 129–142.e6 [CrossRef Medline](#)
16. Azzarelli, R., Hurley, C., Sznurkowska, M. K., Rulands, S., Hardwick, L., Gamper, I., Ali, F., McCracken, L., Hindley, C., McDuff, F., Nestorowa, S., Kemp, R., Jones, K., Göttgens, B., Huch, M., *et al.* (2017) Multi-site neurogenin3 phosphorylation controls pancreatic endocrine differentiation. *Dev. Cell* **41**, 274–286.e275 [CrossRef Medline](#)
17. Beucher, A., Gjernes, E., Collin, C., Courtney, M., Meunier, A., Collombat, P., and Gradwohl, G. (2012) The homeodomain-containing transcription factors Arx and Pax4 control enteroendocrine subtype specification in mice. *PLoS One* **7**, e36449 [CrossRef Medline](#)
18. Gimm, O., Attié-Bitach, T., Lees, J. A., Vekemans, M., and Eng, C. (2000) Expression of the PTEN tumour suppressor protein during human development. *Hum. Mol. Genet.* **9**, 1633–1639 [CrossRef Medline](#)
19. Walker, C. L., Walker, M. J., Liu, N. K., Risberg, E. C., Gao, X., Chen, J., and Xu, X. M. (2012) Systemic bisperoxovanadium activates Akt/mTOR, reduces autophagy, and enhances recovery following cervical spinal cord injury. *PLoS One* **7**, e30012 [CrossRef Medline](#)
20. Dimri, G. P., Lee, X., Basile, G., Acosta, M., Scott, G., Roskelley, C., Medrano, E. E., Linskens, M., Rubelj, I., and Pereira-Smith, O. (1995) A biomarker that identifies senescent human cells in culture and in aging skin *in vivo*. *Proc. Natl. Acad. Sci. U.S.A.* **92**, 9363–9367 [CrossRef Medline](#)
21. Yang, M. H., Hsu, D. S., Wang, H. W., Wang, H. J., Lan, H. Y., Yang, W. H., Huang, C. H., Kao, S. Y., Tzeng, C. H., Tai, S. K., Chang, S. Y., Lee, O. K., and Wu, K. J. (2010) Bmi1 is essential in Twist1-induced epithelial-mesenchymal transition. *Nat. Cell Biol.* **12**, 982–992 [CrossRef Medline](#)
22. Prabhu, S., Ignatova, A., Park, S. T., and Sun, X. H. (1997) Regulation of the expression of cyclin-dependent kinase inhibitor p21 by E2A and Id proteins. *Mol. Cell. Biol.* **17**, 5888–5896 [CrossRef Medline](#)
23. Jensen, J., Heller, R. S., Funder-Nielsen, T., Pedersen, E. E., Lindsell, C., Weinmaster, G., Madsen, O. D., and Serup, P. (2000) Independent development of pancreatic alpha- and beta-cells from neurogenin3-expressing precursors: a role for the notch pathway in repression of premature differentiation. *Diabetes* **49**, 163–176 [CrossRef Medline](#)
24. Chung, J. H., and Eng, C. (2005) Nuclear-cytoplasmic partitioning of phosphatase and tensin homologue deleted on chromosome 10 (PTEN) differentially regulates the cell cycle and apoptosis. *Cancer Res.* **65**, 8096–8100 [CrossRef Medline](#)
25. Hlobilkova, A., Knillova, J., Svachova, M., Skypalova, P., Krystof, V., and Kolar, Z. (2006) Tumour suppressor PTEN regulates cell cycle and protein kinase B/Akt pathway in breast cancer cells. *Anticancer Res.* **26**, 1015–1022 [Medline](#)
26. Brandmaier, A., Hou, S. Q., and Shen, W. H. (2017) Cell Cycle Control by PTEN. *J. Mol. Biol.* **429**, 2265–2277 [CrossRef Medline](#)
27. Wang, S., Jensen, J. N., Seymour, P. A., Hsu, W., Dor, Y., Sander, M., Magnuson, M. A., Serup, P., and Gu, G. (2009) Sustained Neurog3 expression in hormone-expressing islet cells is required for endocrine maturation and function. *Proc. Natl. Acad. Sci. U.S.A.* **106**, 9715–9720 [CrossRef Medline](#)
28. Jensen, J., Pedersen, E. E., Galante, P., Hald, J., Heller, R. S., Ishibashi, M., Kageyama, R., Guillemot, F., Serup, P., and Madsen, O. D. (2000) Control of endodermal endocrine development by Hes-1. *Nat. Genet.* **24**, 36–44 [CrossRef Medline](#)
29. Murata, K., Hattori, M., Hirai, N., Shinozuka, Y., Hirata, H., Kageyama, R., Sakai, T., and Minato, N. (2005) Hes1 directly controls cell proliferation through the transcriptional repression of p27Kip1. *Mol. Cell. Biol.* **25**, 4262–4271 [CrossRef Medline](#)
30. Mutoh, H., Naya, F. J., Tsai, M. J., and Leiter, A. B. (1998) The basic helix-loop-helix protein BETA2 interacts with p300 to coordinate differentiation of secretin-expressing enteroendocrine cells. *Genes Dev.* **12**, 820–830 [CrossRef Medline](#)
31. Smith, S. B., Qu, H. Q., Taleb, N., Kishimoto, N. Y., Scheel, D. W., Lu, Y., Patch, A. M., Grabs, R., Wang, J., Lynn, F. C., Miyatsuka, T., Mitchell, J., Seerke, R., Désir, J., Vanden Eijnden, S., *et al.* (2010) Rfx6 directs islet formation and insulin production in mice and humans. *Nature* **463**, 775–780 [CrossRef Medline](#)
32. Mosmann, T. (1983) Rapid colorimetric assay for cellular growth and survival: application to proliferation and cytotoxicity assays. *J. Immunol. Methods* **65**, 55–63 [CrossRef Medline](#)
33. Itahana, K., Itahana, Y., and Dimri, G. P. (2013) Colorimetric detection of senescence-associated β -galactosidase. *Methods Mol. Biol.* **965**, 143–156 [CrossRef Medline](#)
34. Dahl, J. A., and Collas, P. (2008) A rapid micro chromatin immunoprecipitation assay (microChIP). *Nat. Protocols* **3**, 1032–1045 [CrossRef Medline](#)